Journal of Experimental Botany, Vol. 63, No. 8, pp. 3207–3218, 2012
doi:10.1093/jxb/ers040 Advance Access publication 9 March, 2012
This paper is available online free of all access charges (see http://jxb.oxfordjournals.org/open_access.html for further details)

Journal of Experimental Botany
www.jxb.oxfordjournals.org

RESEARCH PAPER

Live imaging of intra- and extracellular pH in plants using pHusion, a novel genetically encoded biosensor

Kisten Sisse Krag Gjetting*, Cecilie Karkov Ytting*, Alexander Schulz† and Anja Thoe Fuglsang

Department of Plant Biology and Biotechnology, Faculty of Life Sciences, University of Copenhagen and Danish Basic Research Foundation Centre of excellence: Centre for Membrane Pumps in Cells and Disease–PUMPKIN, Thorvaldsensvej 40, 1871 Frederiksberg C, Denmark

* These authors contributed equally to the work.
† To whom correspondence should be addressed. E-mail: als@life.ku.dk

Received 19 December 2011; Revised 23 January 2012; Accepted 26 January 2012

Abstract

Changes in pH are now widely accepted as a signalling mechanism in cells. In plants, proton pumps in the plasma membrane and tonoplast play a key role in regulation of intracellular pH homeostasis and maintenance of transmembrane proton gradients. Proton transport in response to external stimuli can be expected to be finely regulated spatially and temporally. With the ambition to follow such changes live, a new genetically encoded sensor, pHusion, has been developed. pHusion is especially designed for apoplastic pH measurements. It was constitutively expressed in *Arabidopsis* and targeted for expression in either the cytosol or the apoplast including intracellular compartments. pHusion consists of the tandem concatenation of enhanced green fluorescent protein (EGFP) and monomeric red fluorescent protein (mRFP1), and works as a ratiometric pH sensor. Live microscopy at high spatial and temporal resolution is highly dependent on appropriate immobilization of the specimen for microscopy. Medical adhesive often used in such experiments destroys cell viability in roots. Here a novel system for immobilizing *Arabidopsis* seedling roots for perfusion experiments is presented which does not impair cell viability. With appropriate immobilization, it was possible to follow changes of the apoplastic and cytosolic pH in mesophyll and root tissue. Rapid pH homeostasis upon external pH changes was reflected by negligible cytosolic pH fluctuations, while the apoplastic pH changed drastically. The great potential for analysing pH regulation in a whole-tissue, physiological context is demonstrated by the immediate alkalinization of the subepidermal apoplast upon external indole-3-acetic acid administration. This change is highly significant in the elongation zone compared with the root hair zone and control roots.

Key words: Apoplast, *Arabidopsis*, auxin, cytoplasm, GFP, H^+-ATPase, pH homeostasis, pHusion, sensor.

Introduction

Many plant functions such as nutrient and sugar transport across the plasma membrane (PM), cell elongation, and organ development are highly dependent on the ability of individual cells to control pH both in the cytosol and in the apoplast. Furthermore, a number of enzymatic processes are dependent on maintenance of cytosolic pH homeostasis. The cytosol therefore possesses a high passive buffering capacity in order to maintain this homeostasis (Felle, 2001) in the short term. Active processes such as proton exchange with the vacuole and proton production or consumption by metabolic processes maintain homeostasis in the long term (Smith and Raven, 1979; Kurkdjian and Guern, 1989). The cytosolic buffering capacity of plant cells has been reported to be some 10 orders of magnitude larger than the apoplastic buffer capacity. Depending on the cell type and organism, a change in proton concentration of between

Abbreviations: AM, acetoxy methyl ester; BCECF, 2′,7′-bis(2-carboxy-ethyl)-5(6)-carboxy fluorescein; EGFP, enhanced green fluorescent protein; FITC, fluorescein isothiocyanate; IAA, indole-3-acetic acid; MES, 2-(*N*-morpholino)ethanesulphonic acid; MOPS, 3-(*N*-morpholino)propanesulphonic acid; mRFP1, monomeric red fluorescent protein; PI, propidium iodide; PM, plasma membrane; SNARF-1, 5-(and-6)-carboxy seminaphthorhodafluor-1.

25 mM and 90 mM is required to change cytosolic pH by one unit (Plieth *et al.*, 1997; Plieth and Hansen, 1998; Schönknecht and Bethmann, 1998; Oja *et al.*, 1999). In leaves, the apoplastic buffering capacity has been reported to be ~4 mM pH^{-1} (Oja *et al.*, 1999).

Secondary active transport of nutrients is driven by the co-transport with hydrogen ions, or protons (H^+). The activity of these transporters relies on the presence of transmembrane H^+ electrochemical gradients (Palmgren, 2001). Such gradients are established by different primary active H^+ pumping enzymes such as the PM H^+-ATPase, the vacuolar H^+-ATPase, and the H^+-PPases located in the tonoplast and other endomembranes, as well as the PM (Gaxiola *et al.*, 2007).

Tight regulation of pH is also implicated by processes that are regulated by small, controlled fluctuations in pH such as the differential cell expansion in roots in response to gravitational stimulation. Another example is the transient acidification of the cell wall of root hairs to keep them plastic and keeping pace with the volume increase of the root hair cell (Monshausen *et al.*, 2007, 2011). External application of auxin can also elicit rapid Ca^{2+}-dependent pH responses (Monshausen *et al.*, 2011). Evidence is emerging that changing pH levels act as a second messenger or signal in plant cells (Felle, 2001). Protonation of a few amino acids seems to be able to determine gating and hence the water conductance of plant aquaporins during anoxic stress (Tournaire-Roux *et al.*, 2003).

Assessment of pH at the tissue or cell level is often done using pH-sensitive indicator dyes. Dextran-conjugated forms of FITC (fluorescein isothiocyanate) (Hoffmann and Kosegarten, 1995) or Oregon green (Geilfus and Muehling, 2011) can be used for apoplastic pH measurements. For cytosolic pH measurements acetoxy methyl ester (AM) forms of the dyes BCECF [2′,7′-bis(2-carboxy-ethyl)-5(6)-carboxy fluorescein] and SNARF-1 [5-(and-6)-carboxy seminaphthorhodafluor-1] allow loading of the dyes into the cytosol (Gehring *et al.*, 1997; Gonugunta *et al.*, 2008). However, probe loading and inaccessibility of some cell layers, particularly in living root systems, are inherent problems with chemical dyes.

Genetically encoded biosensors such as Cameleon (Miyawaki *et al.*, 1999) and pHluorin (Miesenbock *et al.*, 1998) have been found to be very promising for *in vivo*, non-invasive studies of ion fluctuations in cells. They are mostly based on fluorescent protein variants and have been designed with specificity for a large range of ions and solutes (Chudakov *et al.*, 2010). In contrast to chemical indicators that depend on proper dye loading, such sensors can be expressed in plants and targeted to the cytosol or apoplast. In a pioneering paper using a ratiometric green fluorescent protein (GFP)-based pH sensor, Gao *et al.* (2004) showed that salt and osmotic stress are dealt with differently in *Arabidopsis* roots. Furthermore, genetically encoded sensors have the potential to follow pH changes in specific cell types and subcellular compartments.

This study introduces a novel pH biosensor combining enhanced GFP (EGFP; (Cormack *et al.*, 1996) in a tandem fusion to monomeric red fluorescent protein (mRFP1; Campbell *et al.*, 2002). This EGFP–mRFP1 pH sensor is dubbed 'pHusion' to reflect its tandem concatenation structure. pHusion provides a valuable addition to the toolbox of sensors for pH measurements in living cells. For the present study, stable *Arabidopsis thaliana* transformants were generated with pHusion targeted to the cytosol or the apoplast, respectively. Moreover, a novel and simple system for mounting delicate *Arabidopsis* seedling roots for live microscopy was developed. This system is ideal for perfusion experiments on live roots and has minimal effect on cell integrity and viability, in contrast to mounting methods used previously.

Materials and methods

Sensor construction

mRFP1 was amplified from a pRSETB vector using the left primer oli1879 (5′-TCT AGA AAG GAT CCG ATG GCC TCC TCC GAG G-3′) introducing *Xba*I and *Bam*HI restriction sites, and the right primer oli1864 (5′-G CTA GCG TTA ACG GCG GCG CCG GTG GAG TG-3′) removing the stop codon and introducing *Hpa*I and *Nhe*I restriction sites. The PCR product was then cloned into vector pCR2.1-TOPO (Invitrogen), resulting in the construct pMP1837. EGFP originates from sGFP(S65T) (Chiu *et al.*, 1996) included in the construct pMP1065 generated in the authors' lab. This version of GFP carries the F64L substitution, making it similar to EGFP, but lacks the common H231L silent substitution (Tsien, 1998). EGFP was amplified from pMP1065 with the left primer oli1860 (5′-GCT AGC ATG GTG AGC AAG GGC GAG GAG C-3′) introducing an *Nhe*I site, and the right primer oli1862 (5′-GAG CTC TTA CTT GTA CAG CTC GTC C-3′) introducing a *Sac*I site. The resulting product was cloned into pCR2.1-TOPO, resulting in construct pMP1836. The EGFP *Nhe*I/*Sac*I fragment was subsequently ligated into pMP1837, resulting in construct pMP1848. The resulting construct then consists of mRFP1–AVNAS–EGFP, with the amino acid linker written in single-letter code.

From pMP1848, the mRFP1–EGFP fusion was ligated into pRSETB using *Bam*HI and *Eco*RI restriction sites, resulting in construct pMP1913 used for expression in *Escherichia coli*.

mRFP1–EGFP was topocloned from pMP1848 into the vector pENTR/D-TOPO (Invitrogen), resulting in construct pMP1920. The pH sensor was then recombined into the plant expression vector pK2GW7 (Karimi *et al.*, 2002) by Gateway recombination, resulting in the construct pMP1922 for cytosolic expression in plants.

An apoplastic targeted version of the pH sensor (apo-mRFP1–EGFP) was generated by placing a target signal peptide originating from an *Arabidopsis* chitinase in front of mRFP (Gao *et al.*, 2004). pMP1913 was used as template with the primers oli-1965 (5′-C ACC ATG AAG ACT AAT CTT TTT CTC TTT CTC ATC TTT TCA CTT CTC CTA TCA TTA TCC TCG GCC GAA TCT AGA ATG GCC TCC TCC GAG G-3′) and oli-1862; the targeting signal is underlined in oli-1965. The resulting PCR product was cloned into pENTR/D-TOPO, giving the construct pMP3060. Sequencing confirmed a complete target sequence. Gateway recombination transferred the sensor into pEarleygate100 (Earley *et al.*, 2006), giving the construct pMP3061 for apoplastic expression of the sensor in plants.

The sucrose sensor FLIPSuc90μΔ1 in vector pRSETB was used as template for PCR using the primers oli-2868 (5′-CAC CAT GCG GGG TTC TCA TCA TCA-3′) and oli-2870 (5′-TTA CTT GTA CAG CTC GTC CAT GCC G-3′), which generated a PCR product of ~2800 bp containing the sequence covering enhanced

cyan fluorescent protein (eCFP)–AtThuE–enhanced yellow fluorescent protein (eYFP). This PCR product was cloned into pENTR D-topo. The resulting clone was linearized with *Nru*I, and an LR reaction was performed with the Gateway destination vector pEarleyGate100 (Earley *et al.*, 2006). The destination clone for expression in plants, named pMP3392, was verified by sequencing and restriction digests. The sequence corresponds to the one reported by Lager *et al.* (2006).

In vitro *calibration and testing of perfusion efficiency*

Escherichia coli strain BL.21 expressing either pHusion from the construct pMP1913 or FLIPSuc90μΔ1 in vector pRSETB was grown in 200 ml cultures with LB medium plus ampicillin for 3 d at room temperature, with shaking, in the dark. Cells were harvested at 4 °C and resuspended in 2 ml of lysis buffer: 1 mM MES, pH 7. Cells were frozen and thawed on ice before being lysed by addition of 750 μg ml^{-1} lysozyme and 75 μg ml^{-1} DNase I. Finally cells were sonicated for three to four 15 s cycles on ice. The broken cell debris was removed by centrifugation (15 min at 10 000 *g*) and the supernatant containing the cell lysate was collected and stored at –20 °C. For calibration of pHusion, *E. coli* cell lysate (concentration ~15 mg ml^{-1}) was diluted 10 times in pH buffer, 10 mM each of MES, MOPS, and citrate adjusted to different pH values between 4 and 8 with KOH or HCl. A combination of different compounds in the calibration buffer was chosen to ensure conditions as identical as possible at both high and low pH values. Cell lysate solutions were imaged in the xzy sequential mode using a confocal microscope. EGFP was excited at 488 nm and detected in the green channel at 500–550 nm. mRFP1 was excited at 558 nm and detected in the red channel at 600–630 nm. The perfusion efficiency was tested by twice adding and removing a solution containing purified protein of the sucrose sensor FLIPSuc90μΔ1.

Plant material

Arabidopsis thaliana plants were transformed by floral dipping (Clough and Bent, 1998) in a suspension of the *Agrobacterium tumefaciens* strain C58C1, rifR, carrying either the construct pMP1922 [pHusion, mRFP1–EGFP, pMP3061 (apo-pHusion)] or pMP3392 (FlipSuc90μΔ1). Positive transformants were selected after three generations to ensure stable homozygous lines. Plant lines with high stable expression of the sensors were chosen for subsequent experimentation.

For root experiments, seeds were surface sterilized and stratified on plates containing 1× Murashige and Skoog (MS)+1% sucrose for 2 d, then transferred to a growth chamber with 8 h light/16 h dark conditions for 4–6 d. For studies of mesophyll cells, leaves were used from plants grown on soil for 4–8 weeks with a similar light regime.

Mounting of leaves and roots

Leaves of 1-month-old plants expressing cytosolic pHusion were immobilized on microscope slides using medical adhesive (Hollister, no. 7730), with the abaxial side facing up. The abaxial epidermis and spongy mesophyll were peeled off and a drop of pH 8 buffer was added instantly to avoid desiccation (see Fig. 3F).

Roots of 4- to 6-day-old plants were immobilized either on medical adhesive-coated slides (Chaudhuri *et al.*, 2011), on poly-L-lysine-coated slides (Menzel-Gläser, polysine, J2800AMNZ), in agar, or mounted in water. For agar immobilization, 5 μl of 0.8% agar (Sigma A-1296) were pipetted into a well of a Teflon-coated microscopic slide (Thermo-Scientific, cell-line diagnostic microscope slides/10 wells). After a few seconds, a single seedling was mounted with the tip and lower part of the root on top of the agar. In some experiments, a thin ring of paraffin was added around the well from a 10 ml syringe with a rubber nozzle attached. After 1–2 min, a drop of buffer was placed on top of the sample to avoid desiccation.

Viability test of roots

Roots of 4- to 6-day-old plants were stained with a solution of 40 μM propidium iodide (PI) in water for 5 min and rinsed before image acquisition. Immobilized roots were viewed with a ×40 dipping objective; water-mounted roots were viewed with a ×20 water immersion objective after adding a cover slip. PI was excited at 558 nm and detected between 600 nm and 630 nm.

Perfusion experiments

The perfusion droplet was stabilized between a dipping objective and either the hydrophobic adhesive or Teflon/paraffin. A suction device, connected to a peristaltic pump, was placed with the tip almost touching the dipping drop of the sample. While adding the perfusion solution with a pipette tip from the opposite side of the slide, excess solution was removed by suction, resulting in replacement of the solution. The perfusion solution was either pH buffer (10 mM each of MES, MOPS, and citrate, pH adjusted with KOH, unless indicated otherwise), or a solution of 0.5 mM KCl/0.1 mM $CaCl_2$ with a pH of 5.8 ±1 μM indole-3-acetic acid (IAA). Perfusion experiments were done using ×20 and ×40 dipping objectives.

Imaging

Whole seedlings were imaged using a fluorescence dissection microscope with brightfield and long pass fluorescence emission settings, respectively (excitation 480/40 and emission 515 LP).

Confocal data acquisition was performed on a Leica SP5-X confocal laser scanning microscope (Leica Microsystems, Mannheim, Germany). For pHusion, data were acquired in xyt mode (movie) using line-by-line sequential scanning of EGFP and mRFP1, respectively. EGFP was excited at 488 nm using a white light laser and detected between 500 nm and 550 nm. mRFP1 was excited at either 558 nm or 585 nm (depending on the level of autofluorescence in the tissue) with a white light laser and detected between 600 nm and 630 nm. For the sucrose sensor, CFP was excited with the 458 nm laser line and emission measured in two channels: 470–510 nm (CFP) and 520–560 nm (YFP), respectively. For the viability test, PI was excited with 580 nm and detected between 600 nm and 630 nm. For auxin treatment, the elongation zone recordings were taken 400–800 μm from the root tip, corresponding to the fast elongation zone and the proximal part of the transition zone as defined in Verbelen *et al.* (2006). The mature zone is defined by the presence of fully developed root hairs (>1500 μm from the root tip).

Data analysis

Selection of perfusion experiments for data analysis was done when the optical sections did not show focus shift or drifting during the recording and had a relatively stable initial ratio baseline before any changes of the perfusion buffer. Image data were analysed using the open source software ImageJ http://rsb.info.nih.gov/ij/index.html. First, pixels with saturated intensities were set to zero using a mask. Next background values were subtracted from each channel, based on the average intensity of images acquired from the same tissue in untransformed plants and on the average intensity values in areas without cells. Furthermore, pixels were excluded by masking, if their intensity values fell below a cut-off threshold determined for each channel. Ratio images were generated through pixel-by-pixel calculations, generating floating 32-bit images.

Non-linear fitting of average pixel intensities according to a region of interest (ROI) was done according to a Boltzmann equation using the software GraphPad Prism, generating a sigmoid curve:

$$R = R_{min} + \frac{(R_{max} - R_{min})}{1 + \exp((pKa - pH)/slope)}$$

R is the ratio at a given pH, and R_{max} and R_{min} designate the maximum and minimum ratio obtainable at either high or low pH, respectively. pK*a* is the pH value that gives half the signal; that is, half of the sensor molecules are protonated. Slope describes the steepness of the curve, a larger value giving a shallower curve.

For visual image presentation of ratio images, a pseudocolour look-up table was designed and adjusted to span the dynamic range of the sensor, as calculated from the *in vivo* calibration of the sensor.

Results

*A novel pH sensor, pHusion, works as a ratiometric pH sensor with a pK*a *value of ~6*

A novel pH sensor, pHusion, was generated by tandem fusion of two fluorescent proteins, mRFP1 and EGFP (Fig. 1A). EGFP is very sensitive to differences in pH. High pH of ~7–8 gives the brightest EGFP signal. EGFP fluorescence is gradually quenched at lower pH values and totally quenched at pH values <5. EGFP has previously been shown to have a pK*a* of 6.15 (Llopis *et al.*, 1998). mRFP1 is the monomeric form of DsRed isolated from the red coral *Discosomas* (Campbell *et al.*, 2002). mRFP1 is practically insensitive to pH changes in the physiologically relevant range, with a recorded pK*a* of 4.5 (Campbell *et al.*, 2002). In order to obtain a 1:1 stoichiometry the two fluorescent proteins were linked by a short linker, allowing for ratiometric measurements of pH changes where mRFP1 functions as an intramolecular reference.

With pK*a* values of the two flurophores in the acidic range this sensor was expected to be especially suitable for measurements in the plant apoplast. A titration curve measured on lysates from *E. coli* expressing pHusion with a spectrofluorometer indicated a pK*a* value of 6.2 (data not shown). pHusion was further characterized with confocal microscopy in order to calibrate the excitation and emission settings for imaging with the titration curve. Cell lysates from *E. coli* expressing pHusion were measured at different pH values (Supplementary Fig. S1 available at *JXB* online). This resulted in a pK*a* value of 5.8 (Fig. 1B). Cell lysate was chosen to mimic a cellular environment more closely than purified pHusion. The difference observed in the two

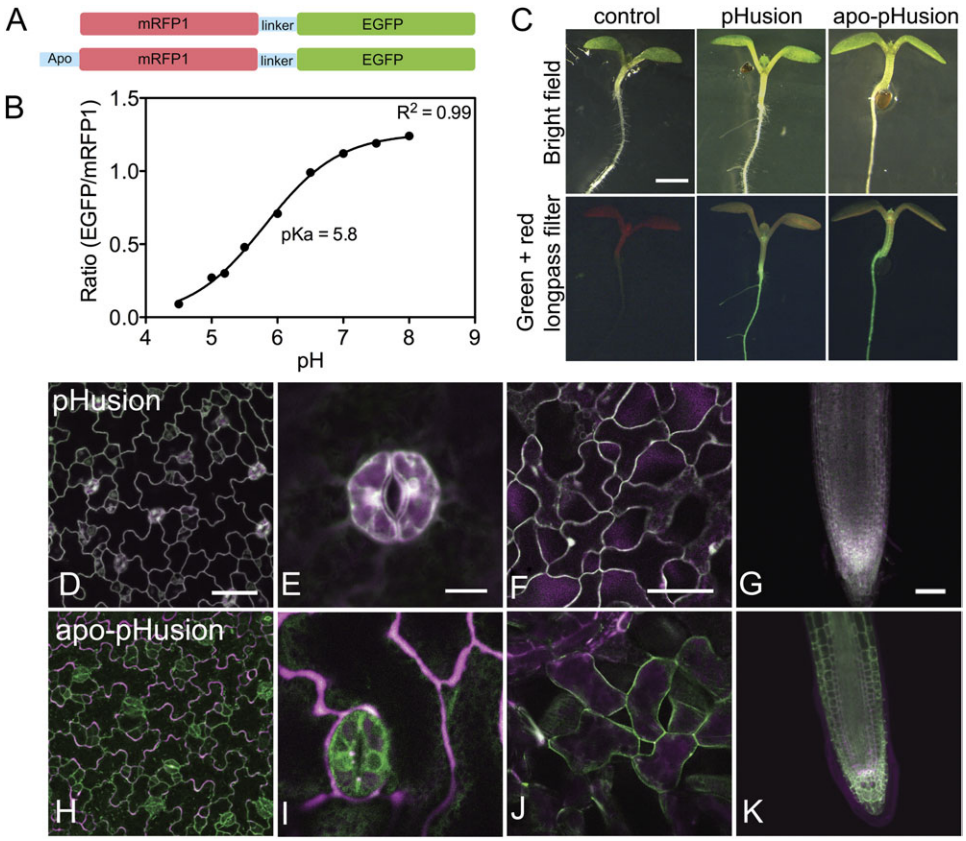

Fig. 1. pHusion reports on pH in all tissues and cell types of *Arabidopsis thaliana*. (A) pHusion sensor constructs. (B) Representative *in vitro* calibration of pHusion using a confocal microscope with the same excitation and emission settings as for pHusion imaging. (C) Expression pattern of pHusion in *Arabidopsis* seedlings expressing either the apoplastic (right panels) or the cytosolic (middle panels) construct compared with the wild-type control (left panels). Scale bar=1 mm in the brightfield control applies to all images in C. (D–K) Confocal overlay images of EGFP (green) and mRFP1 (magenta) channels showing the sensor signal of pHusion (D–G) and apo-pHusion (H–K) in specific tissues and cell types. (D and H) Leaf epidermis; (E and I) guard cells; (F and J) leaf mesophyll; (G and K); root apex. Scale bars: 50 μm (D, F, G, H, J, K); 10 μm (E, I).

obtained pK*a* values can be explained by a difference in the ionic strength in the two dilutions, which will affect the pK*a* value slightly. Estimation of a more precise pK*a* value can be obtained by *in vivo* calibrations (see below).

Quenching of the EGFP signal at low pH is probably due not only to protonation of the fluorophore, but also to an effect of protein aggregation, which was observed in the green and red channel overlay images of *E. coli* pHusion lysate (Supplementary Fig. S1 at *JXB* online). This effect was due either to aggregation of the sensor protein itself or to some factor present in the cell lysate adhering to the sensor, causing aggregation at low pH.

pHusion is expressed well throughout the Arabidopsis *plant body*

Several stable *Arabidopsis* lines were generated expressing pHusion either in the cytosol (pHusion) or targeted to the apoplast (apo-pHusion) by a chitinase targeting sequence (Gao *et al.*, 2004). These lines were tested for expression by fluorescence microscopy, and the lines showing the strongest sensor signal throughout the plant body were chosen for further experimentation. Figure 1C shows wild-type controls and seedlings expressing either the cytosolic or apoplastic version of pHusion observed with a fluorescence dissection microscope. Both plant lines showed strong fluorescence in the green and red spectrum, while autofluorescence in the control was weakly green in the root, and reddish in the aerial parts, corresponding to chlorophyll autofluorescence. There were no obvious morphological differences between seedlings expressing pHusion in either the cytosol or the apoplast compared with the wild type (Fig. 1C) or at later developmental stages (not shown). Accordingly, growth of transformed plants was not affected by either the site of gene insertion or the presence of the sensor.

Confocal image overlays of pHusion EGFP (green) and mRFP1 (magenta) showed a clear and evenly distributed cytosolic and nuclear sensor signal (Fig. 1D–G). Overlay colours revealed only tiny variations in cytosolic pH, independent of the tissue in question: epidermis (Fig. 1D), guard cells (Fig. 1E), leaf mesophyll (Fig. 1F), and root tip (Fig. 1G); all appeared greyish-white with the chosen microscope settings.

Apo-pHusion signal was detected in both the apoplast and the endomembrane system (Fig. 1H–K). This was probably due to accumulation of the sensor in the secretory pathway with the given promoter–signal peptide combination. In contrast to pHusion, apo-pHusion, although evenly distributed in all tissues, showed a more complex pattern of overlay colours. In most cases, an acidic apoplast (dominantly magenta) could be distinguished from the higher pH of the endomembrane compartments (dominantly green), for example in leaf epidermis (Fig. 1H). The guard cells in Fig. 1H and I appear green in the selected intracellular focal plane, revealing the nuclear envelope and a substantial amount of endoplasmic reticulum (ER), contrasting sharply with the acidic (magenta) apoplast. However, signal in the cortical ER network could not always be discriminated from that of the apoplast, making three-dimensional series of optical sections necessary.

It should be noted that the gain settings had to be modified for the apo-pHusion sensor in order to accommodate the broader range of fluorescence intensities in the red channel. Therefore, the overlay colours of pHusion and apo-pHusion are not directly comparable, and the intracellular neutral or slightly alkaline compartments appear greener than in the pHusion signal of the same cell types.

In spongy leaf mesophyll cells (Fig. 1J), from which the lower epidermis was peeled off, the sensor seemed to be localized mainly intracellularly to the cortical ER. Any apoplastic sensor signal was weak. It appears that the apoplastic sensor is easily accessible by and diluted in the imaging buffer when the epidermis is stripped off. Moreover, wounding caused by the stripping procedure probably led to the red intracellular autofluorescence observed in both pHusion- (Fig. 1F) and apo-pHusion- (Fig. 1J) expressing mesophyll cells. A similar red autofluorescence was also detected in wild-type control plants (not shown).

In Fig. 1K, the apoplast around the quiescent centre of the root tip and the future endodermis appeared whitish in the overlay, and slime on the root cap nearly magenta, suggesting characteristic pH microdomains due to cell-specific differences in the apoplastic pH. Images of wild-type plants show only very low background autofluorescence at the settings used (data not shown). As pointed out above, the overlay colours shown in Fig. 1 only represent pH differences within each image. Colours are not comparable between different images due to differences in acquisition settings. For consistent quantification, a much more detailed ratio analysis has to be developed.

Efficiency of the perfusion set-up

In order to follow pH changes in response to external treatments continuously with a confocal microscope, a perfusion system for plant tissues was set up (Fig. 2A). In this set-up any solution is added manually by pipette and excess liquid removed by continuous suction. Before performing *in vivo* perfusion experiments, the efficiency of this system was tested by adding and removing a fluorescent solution (containing the eCFP/eYFP-based FlipSuc90μΔ1 protein) to a microscope slide. It was observed that both accumulation and elimination occurred within 1–3 s, although, in order to eliminate the perfused signal completely, a second wash step was necessary. Hence, this was implemented routinely in the experiments (Fig. 2B).

pHusion responds to pH changes in planta

In planta calibrations of pHusion were performed on mesophyll cells of leaves glued to a microscope slide, with the adaxial surface facing down. Stripping the abaxial epidermis and some of the spongy parenchyma exposed the palisade parenchyma cells. This procedure caused rupture of the PM of some mesophyll cells, which could be used for

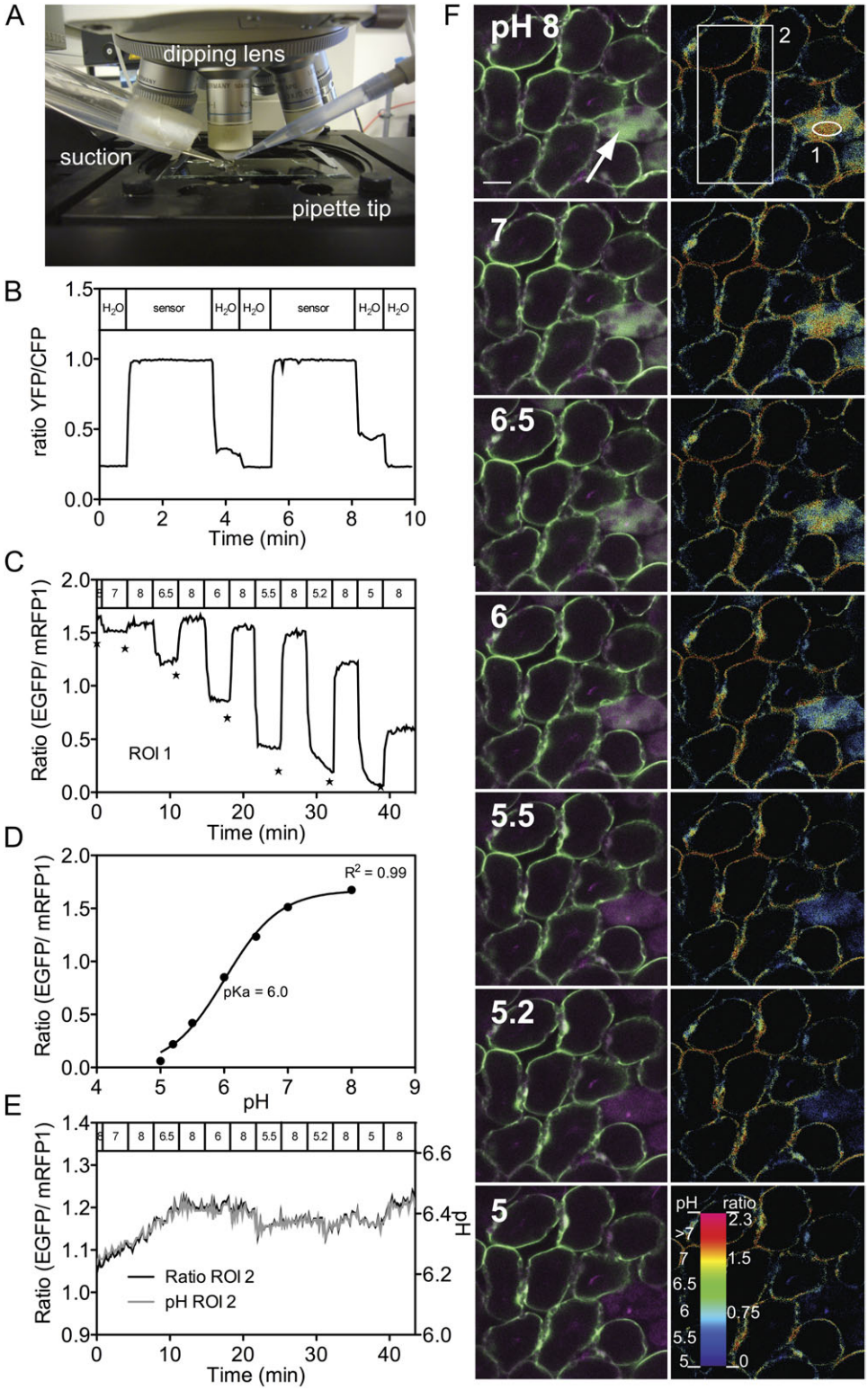

Fig. 2. *In planta* calibration and pH homeostasis of leaf palisade parenchyma cells. (A) Perfusion set-up at the confocal microscope. (B) Perfusion exchange kinetics. A solution of sucrose sensor at pH 7 was repeatedly exchanged with water, and signal intensities were recorded every 3 s. (C–F) Representative experiment of the pH response in leaf palisade parenchyma cells expressing pHusion and treated with a series of buffers of varying pH as indicated. (C) Time course of the effect of pH changes on the average ratio in region of interest 1 (ROI 1) as indicated in the top right panel in F. Stars indicate the data points used for calibration (D) and imaging (F). The buffer pH is indicated above the curve. (D) *In planta* calibration curve. Data points correspond to the values indicated by stars in C. The curve was fitted to a Bolzmann sigmoid curve. (E) Time trace of the effect of pH changes within ROI 2 as outlined in the top right panel in F. The graph depicts both the average ratio (black line) and these values translated into pH using the curve fitted in D (grey line). (F) Optical

in vivo calibration. Calibration was obtained by calculation of the signal intensity ratio of cells with compromised PM and tonoplast during perfusion with a series of different pH buffers (see also time lapse Supplementary Movie S1 at *JXB* online).

Figure 2C–F shows a representative example of such an experiment. The response curve of the cell with compromised membranes (arrow in Fig. 2F) showed a fast and reversible ratio change of sensor fluorescence between pH 8 and pH 5.5 (Fig. 2C). There are indications that the sensor is less stable at pH 5, similar to the observations during *in vitro* calibration, which is here reflected by the fact that it did not reach the initial fluorescence ratio level when returning back to pH 8 (Supplementary Fig. S1 at *JXB* online). The resulting calibration data are shown in Fig. 2D. Fitting of data gave pK*a* values of ~6.0, close to the value obtained by *in vitro* calibration (Fig. 1B).

A ROI covering the cytoplasm of several intact cells shows very little variation in cytosolic pH during buffer treatment (Fig. 2E). According to the *in situ* calibration, the average cytosolic pH in this region is ~6.4. In Fig. 2E, the actual average pixel intensity is shown together with the corresponding pH values calculated on the basis of the fitting function shown in Fig. 2D.

Observations of mesophyll cells after a stripping procedure is a suboptimal approach for studying cellular processes, since some cells are compromised. However, observing intact leaf tissues is challenging since addition of solutes is hindered by the barrier formed by the hydrophobic outer wall of the leaf epidermis. Therefore, measurements on roots were attempted where absorption of solutes from the medium is not hindered by a hydrophobic wall layer.

Medical adhesive affects the viability of seedling root cells

In order to monitor pH during root growth and development, the tissue must be immobilized. Medical adhesive is routinely used for mounting leaves (Hossain *et al.*, 2011; Fig. 2) and roots (Chaudhuri *et al.*, 2008, 2011; Yang *et al.*, 2010) for imaging experiments. Surprisingly, when roots were mounted with medical adhesive, pHusion often showed a blurry distribution, and cellular compartmentation was lost. This indicated that the PM and tonoplast were compromised by the treatment. Figure 3A shows a perfusion experiment with repetitive changes from pH 8 to pH 5.5 while varying the buffer strength between 100 mM and 0.1 mM. The rate of sensor response was directly correlated with buffer strength, demonstrating that the buffer had direct access to the cytosol. Indeed, the rates of cytoplasmic sensor signal changes were similar to those observed with apo-pHusion (Fig. 3A and data not shown).

The integrity of the PM was tested using a standard viability test. The roots were subjected to different mounting procedures including the use of medical adhesive and poly-L-lysine slides. After mounting on slides, the samples were stained for 5 min with PI, a dye that cannot cross intact PMs, and therefore stains the DNA of dead cells only. A clear nuclear PI staining was observed in both medical adhesive- and poly-L-lysine-mounted young roots (Fig. 3B, C), as well as in roots mounted on slides using double-sided tape (data not shown). The PI staining of nuclei was visible not only in the epidermis, but also in deeper root layers. In contrast, very few nuclei were stained in roots mounted in water or in agar (Fig. 3D, E).

In order to avoid adverse mounting conditions, a simple and cheap mounting system was developed for imaging of seedling roots. An agar droplet was placed on a Teflon-coated slide, the part of the root to be observed was immobilized in the agar, and the drop used for dipping objective contact was kept in place simply by surface tension helped by the Teflon layer, or by a thin paraffin barrier (Fig. 3G, lower panel). Using this method, the roots stayed viable for an extended time period (at least a couple of hours), and could be monitored with no movement of the specimen except related to growth (see Supplementary Movie S2 at *JXB* online), which is crucial when following the effects of perfusion imaging experiments.

Damage to cells by the medical adhesive was not only observed in roots expressing pHusion. As another example, the sucrose sensor FLIPSuc90μΔ1 was tested (Lager *et al.*, 2006). This sensor consists of a bacterial periplasmic binding protein linking to eCFP and eYFP, and has a double functionality: upon binding of sucrose, the periplasmic binding protein responds with a conformational change and changes the Förster resonance energy efficiency between eCFP and eYFP. At the same time, it also works as a ratiometric pH sensor, due to the pH sensitivity of eYFP. According to Chaudhuri *et al.* (2008), the amplitude of the pH response due to proton quenching can be in the same range as the substrate-specific response (see their Fig. 7b for the glucose sensor). Perfusion experiments were performed with varying pH buffers on roots mounted with medical adhesive or with the novel agar-based method. As for the pH sensor plants, sucrose sensor signal was blurry in the former case (Fig. 4B), whereas a clear cytosolic signal pattern was observed in the latter case (Fig. 4D). Figure 4A and C shows the eCFP/eYFP ratio over time during perfusion experiments with varying pH buffers. Roots mounted on medical adhesive responded immediately to buffer changes (Fig. 4A). In contrast, pH homeostasis was maintained in root tissue mounted on agar, and the cytosolic pH was stable (Fig. 4C). Subsequent viability tests again confirmed that roots mounted on medical adhesive had compromised PMs (data not shown).

sections of leaf palisade parenchyma cells at the time points indicated by stars in C with the external pH treatment indicated. Left panels show overlays of EGFP (green) and mRFP1 (magenta) channels. Arrow points to cell with compromised plasma membrane and tonoplast. Scale bar: 20 μm. The right panel shows ratio images of the corresponding overlays. ROIs corresponding to the traces of C and E are outlined. The pseudo-colour look-up table shown was adjusted to span the entire ratio signal range as determined in D.

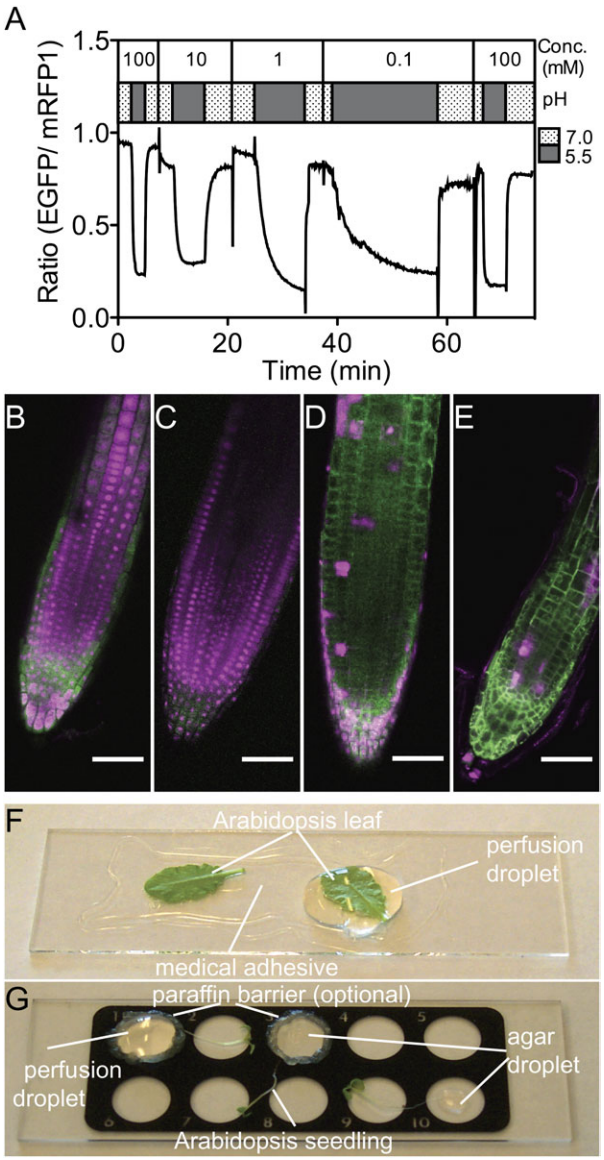

Fig. 3. Medical adhesive destroys the membrane integrity of root cells. (A) Fluorescence ratio change of cytosolic pHusion in *Arabidopsis* root mounted on medical adhesive. The root was subjected to buffers of different pH and different molarities as indicated at the top. The rapidity of ratio changes in the cells is positively correlated with the buffer strength, indicating that the cells have a compromised plasma membrane and reflecting the inherent buffering capacity of the exposed cytoplasm. (B–E) Confocal overlay images showing staining of dead cells with propidium iodide (magenta) in *Arabidopsis* root apexes expressing apo-pHusion (green). Roots were immobilized on medical adhesive (B), on poly-L-lysine (C), with a cover slip (D), and in agar (E). (F and G) Different steps of mounting either a leaf in medical adhesive (F) or a root in a droplet of agar (G). The perfusion droplet is held in place by the hydrophobicity of the medical adhesive and Teflon coating/paraffin, respectively.

In contrast agar-mounted roots were able to grow during the experiment, as seen by increasing cell size in the elongation zone (Supplementary Movie S3 at *JXB* online).

Live imaging of the cytosolic and apoplastic pH responses of roots

Ratio changes of pHusion were analysed in the elongation zone of 5- to 10-day-old roots mounted on agar. Figure 4E (right panel) shows the response of cells expressing pHusion in the cytosol. These results support the observations made in leaf mesophyll cells that cytosolic pH is only slightly influenced by changes in external pH between pH 8 and pH 5.5. No signal change was observed, and all cells remained intact with a sensor signal localized purely to the cytosol and nucleus (Fig. 4G).

The response of apo-pHusion was similarly analysed in intact, elongating root cells, and the sensor responded rapidly and reversibly to external pH changes (Fig. 4E, left panel). Two different ROIs were selected: one placed on the cell wall between epidermis cells (ROI 1) and the other on that between cortex cells (ROI 2). Response to changes of the perfusion buffer was tightly synchronized between the epidermis and cortex cell apoplast, but the dynamic range was smaller in the cortex than in the epidermis (Fig. 4E). This is also reflected in the corresponding calibration curves (Fig. 4E, middle panel). In general, the ratio changes were smaller than those observed in compromised leaf mesophyll cells (Fig. 2C). As noted before, the ratio values observed in different tissues are not directly comparable because of different microscope settings.

Apo-pHusion reports an IAA-stimulated alkalinization of the apoplast in the elongation zone, but not the mature zone of the root

Externally applied IAA has previously been shown to induce a rapid, Ca^{2+}-dependent alkalinization of the root surface spreading shootwards from the elongation root cells, using an external pH-sensitive fluorescein–dextran probe (Monshausen *et al.*, 2011). Seedling roots expressing apo-pHusion were exploited to pursue pH changes inside the root, recording the response in the elongation and mature root zone upon IAA administration. In order to avoid gravitropic effects the roots were left for 10–15 min after mounting before starting the measurements.

Figure 5 shows the effect on live roots of 1 μM IAA in a perfusion solution of 0.5 mM KCl and 0.1 mM $CaCl_2$. The response was recorded in the elongation and mature zone by confocal imaging over 18 min in an image plane exposing inner epidermis cell walls and cortex (corresponding to Fig. 4D). After 1 min, the perfusion solution was reapplied without any changes in response (arrow 1). After an additional 1.5 min, perfusion solution with 1 μM IAA was added (arrow 2). Controls were perfusion solution without IAA. Figure 5 shows that addition of IAA resulted in an immediate alkalinization of the apoplast in the elongation zone. No significant pH changes were detected in the control-treated elongating root cells or in the IAA-treated mature zone. Interestingly, ratio fluctuations were more pronounced in controls and in IAA-treated mature root zones than in the elongation zone, reflecting

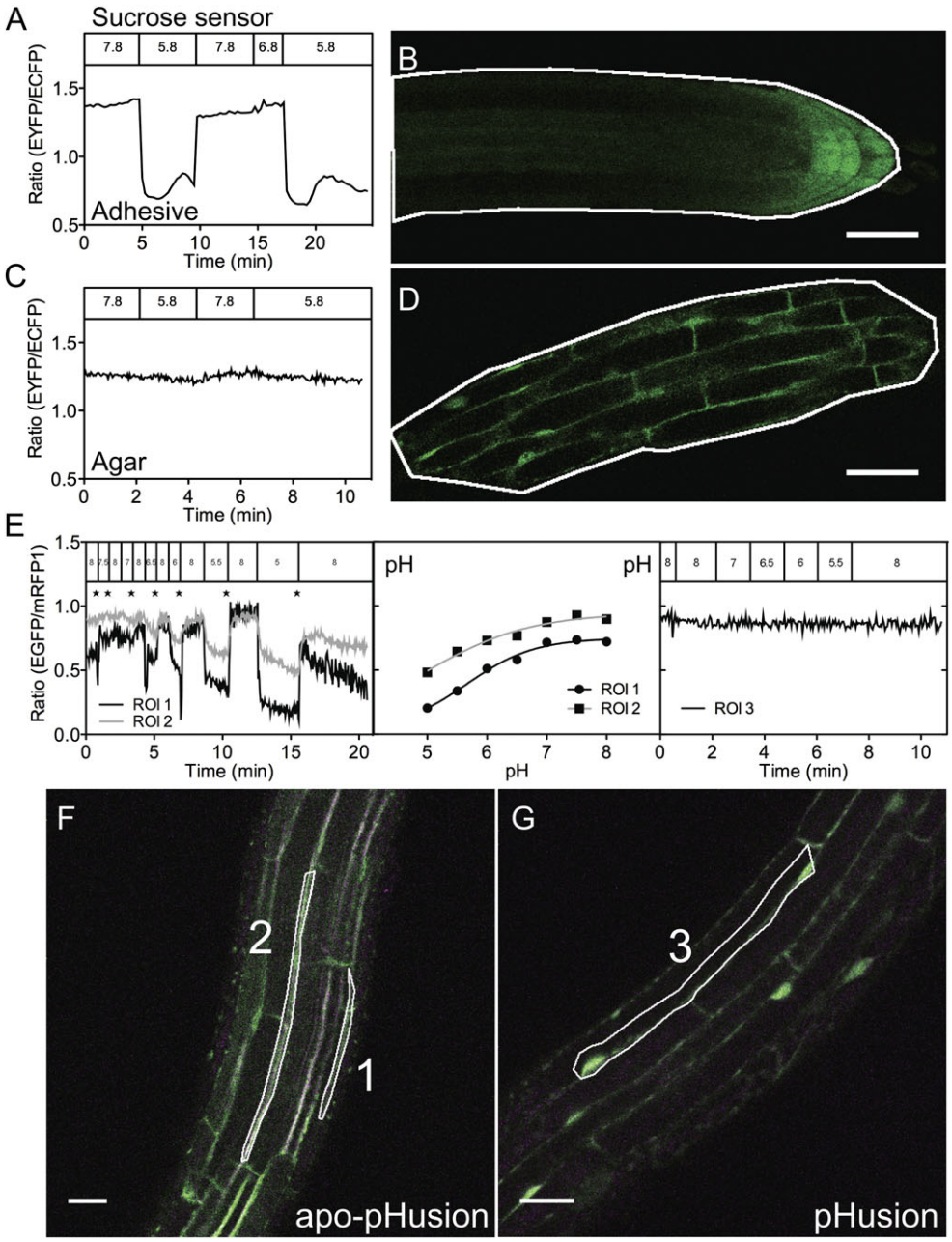

Fig. 4. The pH response of sensors depends on plasma membrane integrity. (A and C) Average pixel ratio changes of the cytosolically expressed sucrose sensor in roots mounted on medical adhesive (A) and on agar (C) within the ROIs outlined in B and D, respectively. (B and D) Sucrose sensor EYFP signal (green) in roots corresponding to the time traces in A and C, respectively. ROIs used for measurements are outlined in white. (E) Response curves of apo-pHusion (left) and pHusion (right) sensor for roots mounted on agar and treated with buffer of different pH as indicated. Titration curves (middle) were generated from the data points marked with stars on the left graph. (F and G) Confocal overlay images of EGFP (green) and mRFP1 (magenta) of the root sections corresponding to the graphs in E. ROIs are outlined in white and numbered according to E. Scale bars (B) and (D): 50 μm; (F) and (G): 20 μm.

dynamic apoplastic pH fluctuations in unregulated root cells, corresponding to the findings of Monshausen *et al.* (2011).

Selected time points were tested by two-way analysis of variance (ANOVA). Highly significant ($P < 0.001$) differences were observed at all time points upon IAA administration in the elongation zone compared with the other groups (Fig. 5, ***). Slightly significant ($P < 0.05$) differences were found at two other time points as indicated by single asterisks in Fig. 5, which may be caused by the previously mentioned highly dynamic baseline of the apoplastic pH.

To test variation and the ability of the cells to respond to pH changes, a calibration was done after each perfusion experiment with pH buffers ranging from pH 7 to 5.5 (data not shown). From the calibration curves obtained, the pH range of the IAA response in the elongation zone could be estimated to be in the range 0.5–0.8 ΔpH units between pH 6 and 7.

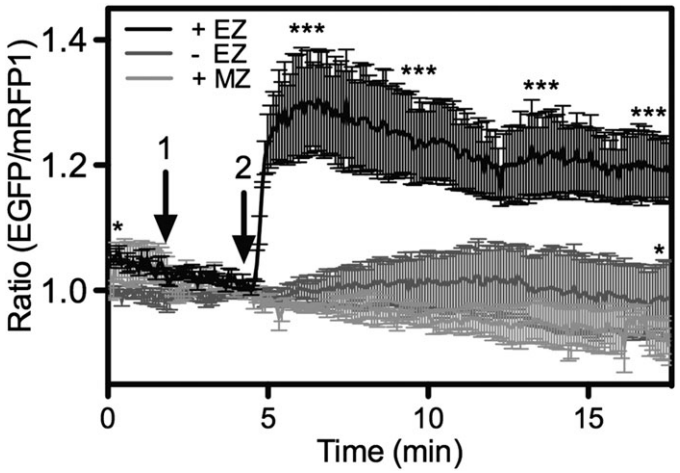

Fig. 5. IAA-induced alkalinization of root cells in the elongation zone. Seedling roots were mounted with agar, covered with a droplet of perfusion solution (0.5 mM KCl/0.1 mM $CaCl_2$), and left for 10–15 min to stabilize before measurements. Roots were viewed in either the elongation zone (EZ) or the mature zone (MZ). Approximately 1 min after starting the measurement, 1 ml of perfusion solution (arrow 1) was added. At arrow 2, the root was again perfused with the solution containing 1 μM IAA (black and dark grey curve) or with the solution only (light grey curve). ROIs were chosen to cover the whole visible root area at the sub-epidermal level as in Fig. 4D. Each treatment was carried out at least in triplicate. Error bars are calculated as the SEM. Changes were highly significant in comparison with control at the time points indicated with *** (see Supplementary Table S1 at *JXB* online).

Discussion

Live measurements of growing plant organs are a challenge, since handling, staining, and mounting for microscopy interfere with cellular physiological processes and are recorded by cells immediately. In roots, gravitropic responses might influence and even override stimuli applied in the experiment, making a vertical set-up of the microscope highly desirable (see Monshausen *et al.*, 2011). The genetically encoded pHusion sensor and a novel mounting technique presented in this study make it possible to record pH changes upon treatment, with minimized impact on the sensitive organ.

pHusion is expressed well throughout the *Arabidopsis* plant body when expressed from the strong constitutive 35S promoter. This is optimal for expression of the cytosolic version of pHusion, since it gives a strong sensor signal. The apoplastic version of the sensor was successfully targeted to the apoplast, but overexpression under the 35S promoter causes additional sensor accumulation in the endomembrane system. While this can be exploited as an internal standard and allows studies on vesicular trafficking in plant cells, it is at the same time also a challenge for apoplastic measurements.

*pK*a *value and challenge of calibration*

With a pK*a* value of ~6, pHusion is well suited for measurements of pH changes in the apoplast of plants. The extracellular cell wall space is more acidic than the cytosol, with pH varying between 5 and 6 (Felle, 2001). Other genetically encoded pH sensors such as the pHluorins (Miesenbock *et al.*, 1998) and the pH-sensitive GFP (S65T/H148D) have pK*a* values of ~7 and 8, respectively, which makes them well suited for detection of cytosolic pH (Elsliger *et al.*, 1999; Schulte *et al.*, 2006). Measurements of root apoplastic pHluorin signal showed pH changes between 6.4 and 6.7 in response to salt treatment (Gao *et al.*, 2004). These authors similarly targeted the sensor to the apoplast using the 35S promoter and a chitinase signal peptide. The higher apoplastic pH values indicated in their experiments, compared with the present results, might reflect the relatively high pK*a* of pHluorins compared with the apoplastic pH, and/or the contribution of the sensor accumulating in the secretory pathway, which is in the neutral pH range. With the high spatial resolution of confocal microscopes the pH contrast of the secretory pathway and the apoplast can be clearly documented in favourable image planes (Fig. 1A). However, even with high magnification, ROIs cannot totally exclude a contribution of cytoplasmic signals.

Importantly, pHusion and other gene-encoded sensors are useful for qualitative observations of pH and relative changes after pH-changing treatments. Exact pH values should, however, be regarded with caution since their reliability depends on the calibration. A number of factors influence the calibration, such as the buffer capacity of the apoplast and the cytosol (see Fig. 3A and Felle, 2001). A comparison of the pHusion response curves of the compromised mesophyll cells and root cells shows a difference in the maximal achievable ratio change of the sensor between pH 8 and 5 that is much smaller in the root measurements. A considerable signal contribution from endomembrane systems can account for this. With the chosen magnifications and the given resolution of the imaging system, a contribution of the 'close to neutral' endomembrane system to the apoplastic signal cannot be excluded, causing a decrease in the dynamic range of the sensor (Fig. 4B). Moreover, calibrations become particularly unreliable when the measured values are close to the end of the linear range of any sensor (Benjaminsen *et al.*, 2011).

A novel mounting method

A novel method is presented for immobilizing *Arabidopsis* seedling roots before imaging. It was developed because the medical adhesive routinely used for live imaging of leaves turned out to be unsuitable for roots, compromising the PM as evidenced by a standard test for cell viability (Fig. 3C) (Huang *et al.*, 1986). Mounting roots on poly-L-lysine-coated slides also caused impaired cell viability. This might be due either to mechanical stress during mounting, as root cells immediately stick to the adhesive on contact, or to the chemical nature of the medical adhesive. The adhesive contains formaldehyde, a compound listed as a possibly hazardous decomposition compound (Hollister, 2010). There are several requirements for the mounting procedure in order to perform ratiometric pH measurements on roots.

First of all roots should be totally immobilized, yet alive and able to grow. At the same time, the root tissues should be directly accessible to the perfusion medium, which excludes sowing the seeds on glass cover slips in a layer of nutrient agar medium (Fricker *et al.*, 1999). By placing the root in a droplet of low concentration agar, root cells could be kept alive for hours. No drifting of the specimen during perfusion was observed over 13 min, which is a prerequisite for quantitative measurements at the subcellular level (Supplementary Movie S2 at *JXB* online).

pH response in the cytosol and apoplast to apoplastic stimuli

In the present study, pH shifts and IAA were applied as external stimuli to follow cellular responses in leaf and root tissue. Steep pH changes applied by perfusing the immobilized specimens had surprisingly small effects on the cytosolic pH value of the self-reporting tissue, both in the leaf mesophyll and in subepidermal root tissue (Figs 2 and 4, respectively). This was not only valid for the pHusion when expressed in the cytosol, but also for the bi-functional sucrose sensor (Fig. 4C). In contrast, the apoplastic pH changes immediately upon change of the perfusion buffer, and is synchronized when comparing the response in the epidermis and the subepidermal cortex layer (Fig. 4E). Both the cytoplasm and the apoplast have a certain buffering capacity. The cytoplasm became accessible for measurements when the roots of pHusion plants were immobilized with the medical glue. Sensor ratio changes were slower to be correlated with smaller concentrations of the perfusion buffer (Fig. 3A). In the case of apo-pHusion plants, the root apoplast was directly accessible to the perfusion buffer. However, the sensor approached the final ratio only after 1–2 min as seen in the cortex ROI, even though the initial response was synchronized with that in the epidermis (Fig. 4E).

Using pH- and calcium-sensitive probes, Monshausen *et al.* (2011) elegantly demonstrated an almost instantaneous alkalinization response to auxin at the root surface mediated by cytosolic calcium influx. They substantiated that gravitropic signal transmission is associated with asymmetric Ca^{2+} distribution originating in the root apex and coordinating the elongation zone alkalinization and thus the growth response in a manner distinct from and faster than the TIR1 auxin signalling pathway. With the apo-pHusion sensor, the effects of external IAA application to living roots could be reproduced. Expression of the sensor throughout the root allowed it to record the alkalinization after IAA application at the cellular level inside the root; that is, in the subepidermal tissue layer. This alkalinization seemed to be limited to the elongation zone and was not evident in the root hair zone.

Conclusion

The novel pHusion sensor is highly suitable for dynamic pH measurements in various plant tissues at the cellular and subcellular level. A prerequisite for an appropriate use of such sensors for physiologically relevant live recordings is adequate mounting and handling methods, which is demonstrated here with an improved immobilization technique suitable in particular for seedling roots and allowing for easy exchange of the external buffer solution. Response of pH changes and external IAA administration is shown to be rapid in the apoplast. According to pHusion sensor readings upon external pH changes, the cytosol has an efficient homeostasis system, maintaining the pH at neutral values. Future experiments will allow discrimination of the mechanisms of short-term and long-term homeostasis.

Supplementary data

Supplementary data are available at *JXB* online.

Figure S1. Lysates from *E. coli* expressing pHusion used for *in vitro* calibration. The images show aggregation of sensor protein in buffers of low pH value.

Movie S1. Time lapse *of in planta* calibration corresponding to Fig. 2.

Movie S2. Time lapse of apoplastic pHusion expression (overlay of GFP and RFP) and the transmission channel in living root cells corresponding to Fig. 4F.

Movie S3. Time lapse of a growing root tip mounted with agar.

Table S1. Significance levels of two-way ANOVA carried out between all the treatments in Fig. 5.

Acknowledgements

This work was supported by: Danish Research Council for Technology and Production (grant no. 274-07-0172; LiMeS project); FOBI (Research School for Biotechnology, KU-LIFE). We are grateful to Wolf Frommer for providing FLIPSuc90μΔ1 and to Roger Tsien for mRFP1. Imaging data were acquired at the Center for Advanced Bioimaging (CAB) Denmark, University of Copenhagen. We wish to thank Michael Hansen for technical assistance and intellectual sparring.

References

Benjaminsen RV, Sun H, Henriksen JR, Christensen NM, Almdal K, Andresen TL. 2011. Evaluating nanoparticle sensor design for intracellular pH measurements. *ACS Nano* **5,** 5864–5873.

Campbell RE, Tour O, Palmer AE, Steinbach PA, Baird GS, Zacharias DA, Tsien RY. 2002. A monomeric red fluorescent protein. *Proceedings of the National Academy of Sciences, USA* **99,** 7877–7882.

Chaudhuri B, Hörmann F, Frommer WB. 2011. Dynamic imaging of glucose flux impedance using FRET sensors in wild-type Arabidopsis plants. *Journal of Experimental Botany* **62,** 2411–2417.

Chaudhuri B, Hörmann F, Lalonde S, Brady SM, Orlando DA, Benfey P, Frommer WB. 2008. Protonophore- and pH-insensitive glucose and sucrose accumulation detected by FRET nanosensors in Arabidopsis root tips. *The Plant Journal* **56,** 948–962.

Chiu W, Niwa Y, Zeng W, Hirano T, Kobayashi H, Sheen J. 1996. Engineered GFP as a vital reporter in plants. *Current Biology* **6,** 325–330.

Chudakov DM, Matz MV, Lukyanov S, Lukyanov KA. 2010. Fluorescent proteins and their applications in imaging living cells and tissues. *Physiological Reviewas* **90,** 1103–1163.

Clough SJ, Bent AF. 1998. Floral dip: a simplified method for Agrobacterium-mediated transformation of Arabidopsis thaliana. *The Plant Journal* **16,** 735–743.

Cormack BP, Valdivia RH, Falkow S. 1996. FACS-optimized mutants of the green fluorescent protein (GFP). *Gene* **173,** 33.

Earley KW, Haag JR, Pontes O, Opper K, Juehne T, Song K, Pikaard CS. 2006. Gateway-compatible vectors for plant functional genomics and proteomics. *The Plant Journal* **45,** 616–629.

Elsliger MA, Wachter RM, Hanson GT, Kallio K, Remington SJ. 1999. Structural and spectral response of green fluorescent protein variants to changes in pH. *Biochemistry* **38,** 5296–5301.

Felle HH. 2001. pH: signal and messenger in plant cells. *Plant Biology* **3,** 577–591.

Fricker MD, Plieth C, Knight H, Blancaflor E, White NS, Gilroy S. 1999. Fluorescence and luminescence techniques to probe ion activity in living plant cells. In: Mason WT, ed. *Fluorescent and luminescent probes for biological activity. A practical quide to technology for quantitative real-time analysis*. New York: Academic Press, 569–596.

Gao D, Knight MR, Trewavas AJ, Sattelmacher B, Plieth C. 2004. Self-reporting Arabidopsis expressing pH and [Ca^{2+}] indicators unveil ion dynamics in the cytoplasm and in the apoplast under abiotic stress. *Plant Physiology* **134,** 898–908.

Gaxiola RA, Palmgren MG, Schumacher K. 2007. Plant proton pumps. *FEBS Letters* **581,** 2204.

Gehring CA, Irving HR, McConchie R, Parish RW. 1997. Jasmonates induce intracellular alkalinization and closure of Paphiopedilum guard cells. *Annals of Botany* **80,** 485–489.

Geilfus C-M, Muehling KH. 2011. Real-time imaging of leaf apoplastic pH dynamics in response to NaCl stress. *Frontiers in Plant Science* **2,** 13.

Gonugunta VK, Srivastava N, Puli MR, Raghavendra AS. 2008. Nitric oxide production occurs after cytosolic alkalinization during stomatal closure induced by abscisic acid. *Plant, Cell and Environment* **31,** 1717–1724.

Hoffmann B, Kosegarten H. 1995. FITC–dextran for measuring apoplast pH and apoplastic pH gradients between various cell types in sunflower leaves. *Physiologia Plantarum* **95,** 327–335.

Hollister. 2010. Material Safety Data Sheet. Hollster Medical Adhesive Spray. http://www.hollister.com/us/files/pdfs/msds/7730.pdf.

Hossain MA, Munemasa S, Uraji M, Nakamura Y, Mori IC, Murata Y. 2011. Involvement of endogenous abscisic acid in methyl jasmonate-induced stomatal closure in Arabidopsis. *Plant Physiology* **156,** 430–438.

Huang CN, Cornejo MJ, Bush DS, Jones RL. 1986. Estimating viability of plant protoplasts using double and single staining. *Protoplasma* **135,** 80–87.

Karimi M, Inzé D, Depicker A. 2002. GATEWAY vectors for Agrobacterium-mediated plant transformation. *Trends in Plant Science* **7,** 193–195.

Kurkdjian A, Guern J. 1989. Intracellular pH: measurement and importance in cell activity. *Annual Review of Plant Physiology and Plant Molecular Biology* **40,** 271–303.

Lager I, Looger LL, Hilpert M, Lalonde S, Frommer WB. 2006. Conversion of a putative Agrobacterium sugar-binding protein into a FRET sensor with high selectivity for aucrose. *Journal of Biological Chemistry* **281,** 30875–30883.

Llopis J, McCaffery JM, Miyawaki A, Farquhar MG, Tsien RY. 1998. Measurement of cytosolic, mitochondrial, and Golgi pH in single living cells with green fluorescent proteins. *PNAS* **95,** 6803–6808.

Miesenbock G, De Angelis DA, Rothman JE. 1998. Visualizing secretion and synaptic transmission with pH-sensitive green fluorescent proteins. *Nature* **394,** 192–195.

Miyawaki A, Griesbeck O, Heim R, Tsien RY. 1999. Dynamic and quantitative Ca^{2+} measurements using improved cameleons. *Proceedings of the National Academy of Sciences, USA* **96,** 2135–2140.

Monshausen GB, Bibikova TN, Messerli MA, Shi C, Gilroy S. 2007. Oscillations in extracellular pH and reactive oxygen species modulate tip growth of Arabidopsis root hairs. *Proceedings of the National Academy of Sciences, USA* **104,** 20996–21001.

Monshausen GB, Miller ND, Murphy AS, Gilroy S. 2011. Dynamics of auxin-dependent Ca^{2+} and pH signaling in root growth revealed by integrating high-resolution imaging with automated computer vision-based analysis. *The Plant Journal* **65,** 309–318.

Oja V, Savchenko G, Jakob B, Heber U. 1999. pH and buffer capacities of apoplastic and cytoplasmic cell compartments in leaves. *Planta* **209,** 239–249.

Palmgren MG. 2001. PLANT PLASMA MEMBRANE H^+-ATPases: powerhouses for nutrient uptake. *Annual Review of Plant Physiology and Plant Molecular Biology* **52,** 817–845.

Plieth C, Hansen UP. 1998. Cytosolic Ca^{2+} and H^+ buffers in green algae: a reply. *Protoplasma* **203,** 210–213.

Plieth C, Sattelmacher B, Hansen UP. 1997. Cytoplasmic Ca^{2+}–H^+-exchange buffers in green algae. *Protoplasma* **198,** 107–124.

Schulte A, Lorenzen I, Bottcher M, Plieth C. 2006. A novel fluorescent pH probe for expression in plants. *Plant Methods* **2,** 7.

Schönknecht G, Bethmann B. 1998. Cytosolic Ca^{2+} and H^+ buffers in green algae: a comment. *Protoplasma* **203,** 206–209.

Smith FA, Raven JA. 1979. Intracellular pH and its regulation. *Annual Review of Plant Physiology* **30,** 289–311.

Tournaire-Roux C, Sutka M, Javot H, Gout E, Gerbeau P, Luu D-T, Bligny R, Maurel C. 2003. Cytosolic pH regulates root water transport during anoxic stress through gating of aquaporins. *Nature* **425,** 393–397.

Tsien RY. 1998. The green fluorescent protein. *Annual Review of Biochemistry* **67,** 509–544.

Verbelen JP, De Cnodder T, Le J, Vissenberg K, Baluska F. 2006. The root apex of Arabidopsis thaliana consists of four distinct zones of growth activities: meristematic zone, transition zone, fast elongation zone and growth terminating zone. *Plant Signaling and Behavior* **1,** 296–304.

Yang H, Bogner M, Stierhof Y-D, Ludewig U. 2010. H^+-independent glutamine transport in plant root tips. *PLoS ONE* **5,** e8917.